

Brief Analysis for Future Urban Water Stress & Rainwater Capture in the Mediterranean Region

Graduate School of Climate Studies

University of Bern

Name: Leonardo Quirino Olvera

Student Number: 20-109-609

Course: Climate Risk Assessment

Professor: Prof. Dr. Olivia Romppainen-Martius

1 Introduction

As the human species continues to exist it will require a minimum of natural resources to satisfy its physical needs such as food, air, clothing, shelter, and water. This puts pressure on the existing available resources to satisfy these needs; increasingly, a greater percentage of people are going to live in urban areas. According to the UN (2022) the percentage of the world population is expected to expand from a current 55 % to a 68 % by 2050. So, in an ever-changing world, it becomes crucial to construct and adapt our cities to live in a sustainable manner. Expecting the urban ratio of population to grow, it gains greater importance to adapt our cities for a changing climate. The IPCC (2022) mentions that integrated sustainable urban planning can have mitigation and adaption benefits (medium confidence). Amongst these are water-sensitive measures that may reduce stress on urban sewage systems, reducing flood risks (high confidence) and, in the case of rainfall capture, could complement the ways to obtain water.

The percentage of water resource designated to household use in Europe is 18 % (Kristensen et al., 2004). Within Europeans, the inhabitants of Southern Europe are whom have a larger portion living under water stress year wide. Specially during the summer, 70 % of its residents live in seasonal water stress Zhongming et al. (2009). Considering Spain as an example, the Instituto Nacional de Estadística de España (2018) says that the average domestic water consumption for a Spanish citizen is **133 lts** per day.

1.1 Objectives

As first analysis this paper aims to:

1. Evaluate the current and future rain patterns in the Mediterranean basin.
 - (a) Assess the number and changes in the Consecutive Dry Days index.
 - (b) Analyze feasibility of rainwater capture for at least one city in the region.

2 Data

2.1 CORDEX - CLMcom

For this experiment the CORDEX - ICHEC-EC-EARTH_CLMcom-CCLM4-8-17_v1 was used. It was developed by the Climate Limited-area Modelling Community (CLM-Community) and has “unrestricted” terms of use according to ESGF CORDEX (2022). This particular Coordinated Regional Downscale Experiment (CORDEX) for Europe has eight climate variables and a spatial resolution of $0.1 \times 0.1^\circ$. This includes a **Period from 1971 - 2000** and the future emission of **RCP 8.5** scenario for the **Period of 2071 - 2100**, which assumes an additional radiative forcing of 8.5 W/m^2 for the year 2100.

2.2 Units

The variable selected to work with was precipitation with units $\langle \text{kg} \cdot \text{m}^{-2} \text{s}^{-1} \rangle$, so it was necessary to convert:

$$\langle \frac{\text{kg}}{\text{m}^2 \cdot \text{s}} \rangle = \frac{\text{kg}}{\text{m}^2} \frac{(60 \cdot 60 \cdot 24) \cdot \text{s}}{\text{day} \cdot \text{s}} = \langle \text{mm/day} \rangle \quad (1)$$

From Equation 1 we obtain a more intuitive working variable for precipitation mm/day .

2.3 Population Data

The population data used in this study was obtained from the History Database of the Global Environment (HYDE_3.1) Model mentioned by Klein Goldewijk et al. (2010). It is a land mask that portrays population density at a spatial resolution of also $0.1 \times 0.1^\circ$. Existing the current and future relevance mentioned in the introduction, it was decided to plot urban areas with a $\text{POP} \geq 500,000$ population density for the years 2020 and 2093.

2.4 Area of Study

The area of study is reduce to what considered the Mediterranean inland sea, its surroundings and its population, as shown in Figure 1. It comprises **LATITUDES (MAX: 45 and MIN: 35 °)** and **LONGITUDES (MAX: 37 and MIN: -10 °)**, the Eastern Coast of the Middle East, Northern Africa and Southern Europe.

Three cities were briefly studied and their data were extracted using *method='nearest'*. Table 1 shows which cities and their position:

Table 1: Cities and their geographical positions.

City	Latitude	Longitud
Madrid, Spa.	40.416667	-03.702500
Rome, Ita.	41.893333	12.482778
Cairo, Egp.	30.044444	31.235833

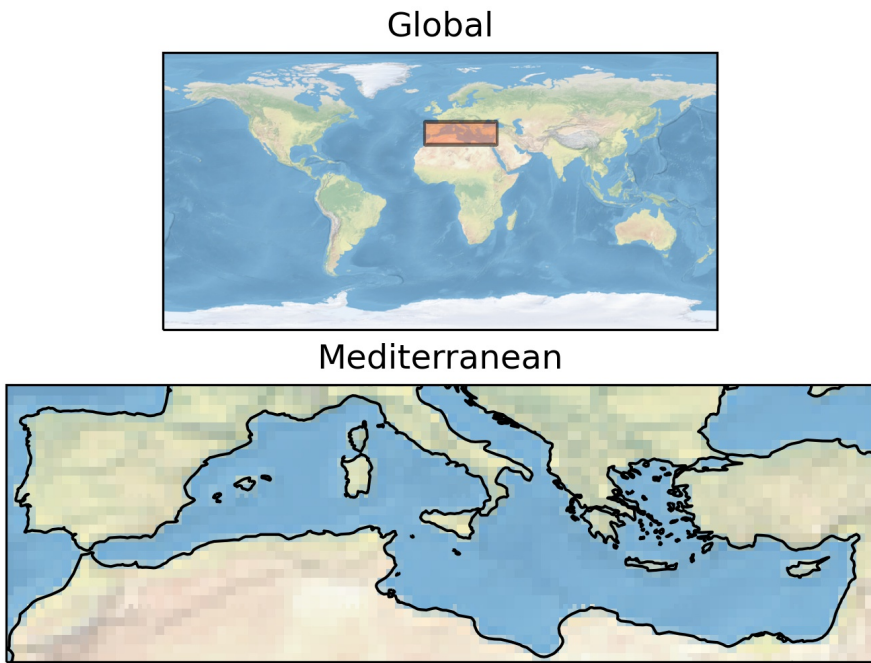


Figure 1: Geographic Focus Area: Mediterranean.

3 Methods

3.1 Climatological Normals of Precipitation

To obtain the corresponding climatological normals for precipitation, it is required of a 30-year consecutive period as its standard in the *World Organization Guidelines on the Calculations of Climate Normals* (WMO, 2017). The data was resampled on a monthly basis and sum for each corresponding day belonging to each month by using `resample(time = 'M').sum()`. This allowed to obtain three different climatological normals:

- 30-year Climatological Normals (Yearly Average Precipitation),
- Climatological Normals for each month, and
- Seasonal Normals (Summer and Winter) for each 30-year period.

This was done for the 30-year reference time span (1971 - 2000 & 2071 - 2100).

NOTE: for any anomaly or difference calculation is the period (2071 - 2100 RCP 8.5) MINUS period (1971 - 2000).

3.2 Variance Maps and Correlation

With the database resampled into monthly timesteps and obtaining the seasonal mean, it was possible to calculate the seasonal variance of the whole period with `var('season')` for each node.

3.2.a) Correlation and Statistical Significance

Once the Anomaly (1971 - 2000 & 2071 - 2100) for Average Precipitation and the Anomaly of the Seasonal Variance were calculated. They were correlated with $xr.corr(anom_prcp, anom_var_prcp)$; $r_{prcp} \approx 0.3039$. The $H_0 : \rho = 0$ was tested by a t-distribution:

$$t = r_{prcp} \sqrt{\frac{n - 2}{1 - r_{prcp}^2}} \quad (2)$$

Which from Eq. 2, $n = 151 \cdot 471 = 71121$ points, so the degrees of freedom are $df = n - 2 = 71119$. $t = 85.082$:

$$p = Pr(|t_{71119}| > 85.082) \quad (3)$$

Given Eq. 3, $p = < 0.0001$ it is concluded that the null hypothesis H_0 is rejected. Therefore there is enough evidence to claim that $\rho \neq 0$ at the $\alpha = 0.001$ significance level.¹

3.3 Consecutive Dry Days Index

The annual number of Consecutive Dry Days (CDD) is index that calculates the longest time span of days that does not rain. CDDs are obtained for the two studied periods (1971-2000 and 2021-2050) was obtained with a xclim function (Ouranos Inc. et al., 2022). Subsequently, their histograms and the average annual number of CDD for both periods were determined.

3.4 Rainwater Catcher

For the rainwater catcher percentage it was first necessary to obtain a monthly average for water consumption per capita for domestic use. The Spanish citizen average consumption was used for the case study, this is due to the main discussion was on the rainwater in the city of Madrid. However, it is understood that each nation's average consumption varies due culture, wealth, policies, etc. The given domestic consumption before mentioned by a Spanish citizen is $133\text{lt}/\text{day}$ per capita:

$$W_{mean} = \frac{133 \cdot 365}{12} = 4045.42 \text{ lt/month} \quad (4)$$

The result from Eq. 4 is $W_{mean} = 4045.42 \text{ lt/month}$ which are the amount of liters of water a person would have to capture to cover 100% of their needs. If we were to assume a hypothetical rainwater catcher of 10 m^2 :

$$W_{percent} = \frac{W_{mon_i} \cdot 10}{W_{mean}} \cdot 100 \quad (5)$$

Eq. 5 is an index that represents the percentage of the average monthly water consumption per person is captured by an 10 m^2 in a given month at a given spot. A conceptual example is shown in Figure 2

¹p-value calculator <https://mathcracker.com/correlation-coefficient-significance>

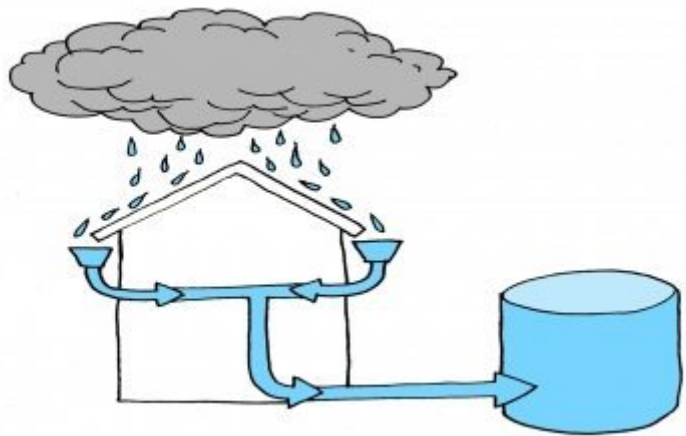


Figure 2: Conceptual Rainwater Catcher.

4 Results

4.1 Reference Period (1971 - 2000)

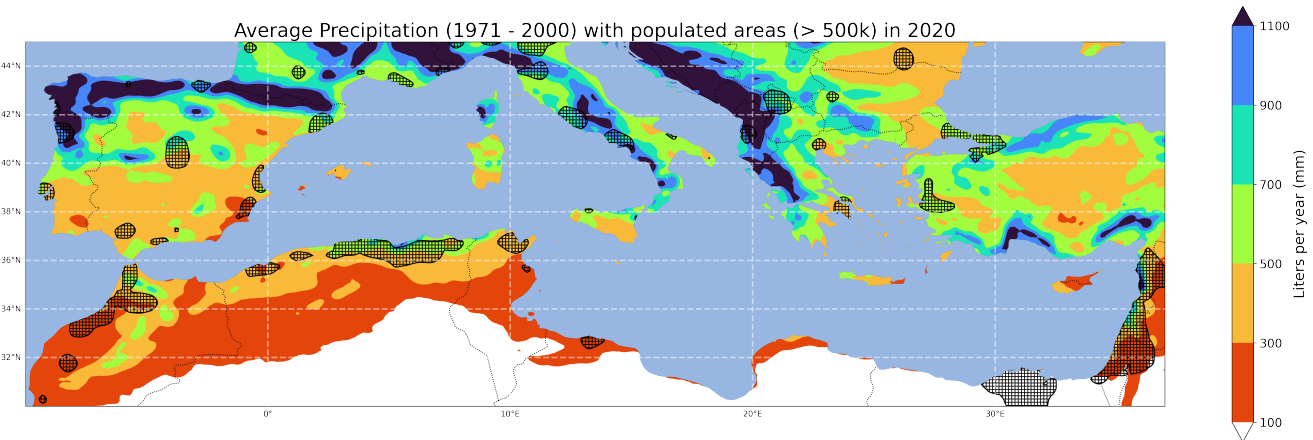


Figure 3: Yearly Average Precipitation (1971 - 2000) with Population over 500,000 in 2020.

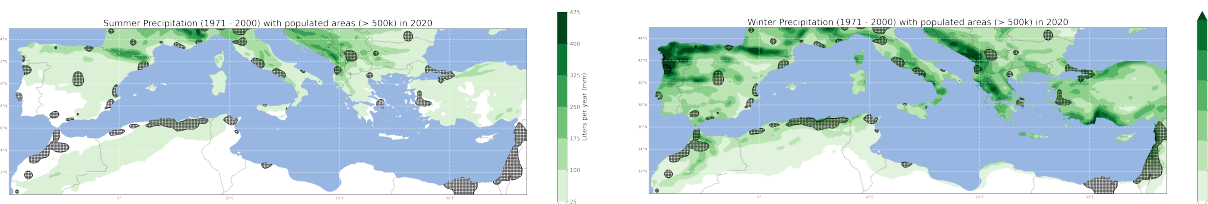


Figure 4: Average Summer Precipitation (1971 - 2000). Figure 5: Average Winter Precipitation (1971 - 2000).
Summer (June, July and August) and Winter (December, January and February) with Population over
500,000 in 2020.

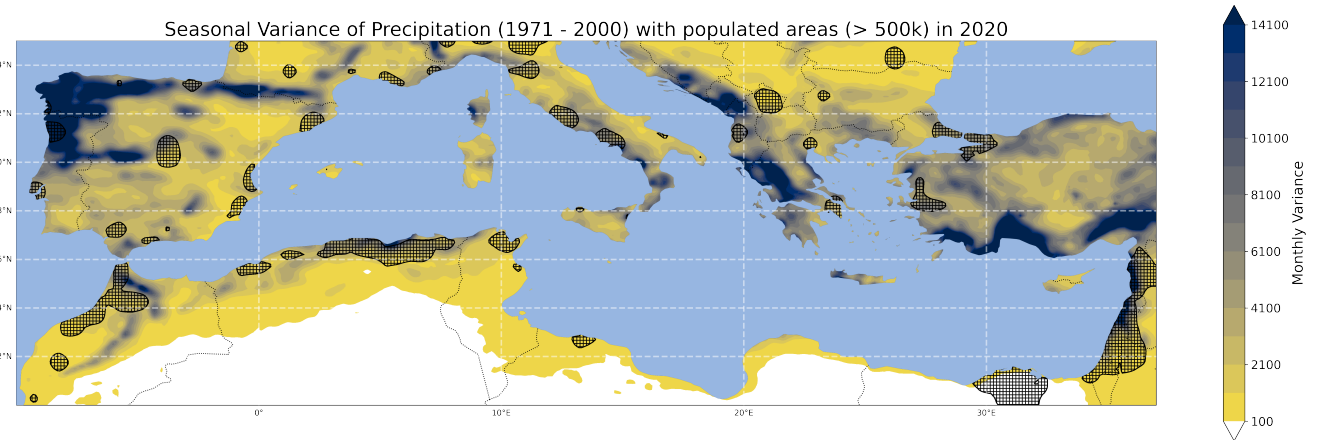


Figure 6: Average Seasonal Precipitation Variance (1971 - 2000) with Population over 500,000 in 2020.

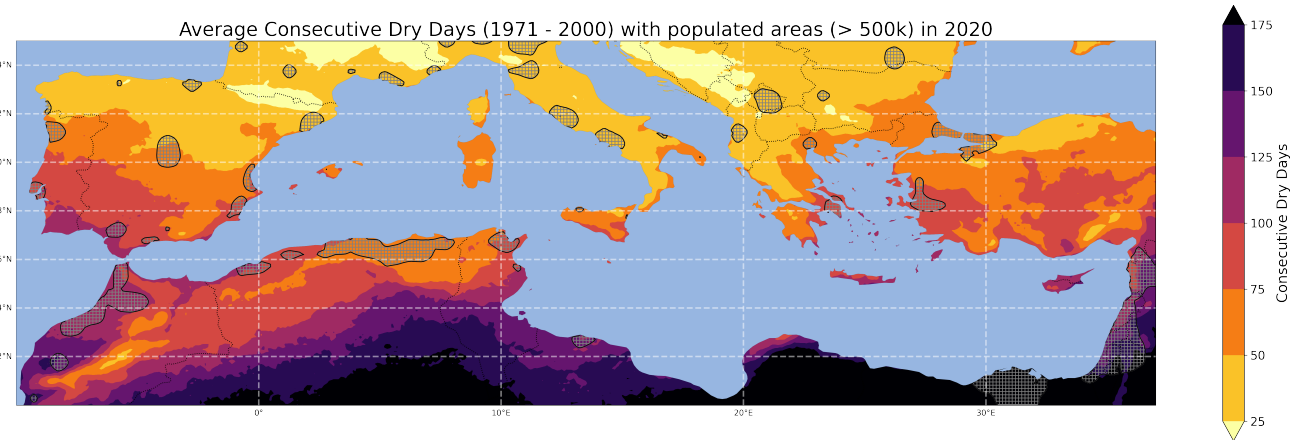


Figure 7: Average Consecutive Dry Days in a Year (1971 - 2000) with Population over 500,000 in 2020.

4.2 Comparisons RCP 8.5 (2071 - 2100) and Reference Period (1971 - 2000)

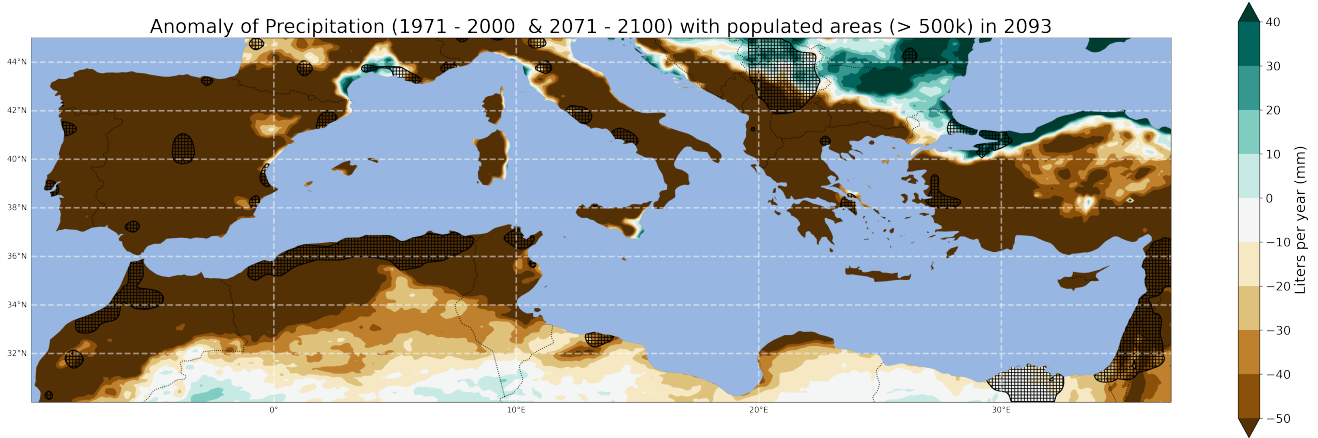


Figure 8: Anomaly of Yearly Average Precipitation (1971 - 2000 2071 - 2100) with Population Projection over 500,000 in 2093.

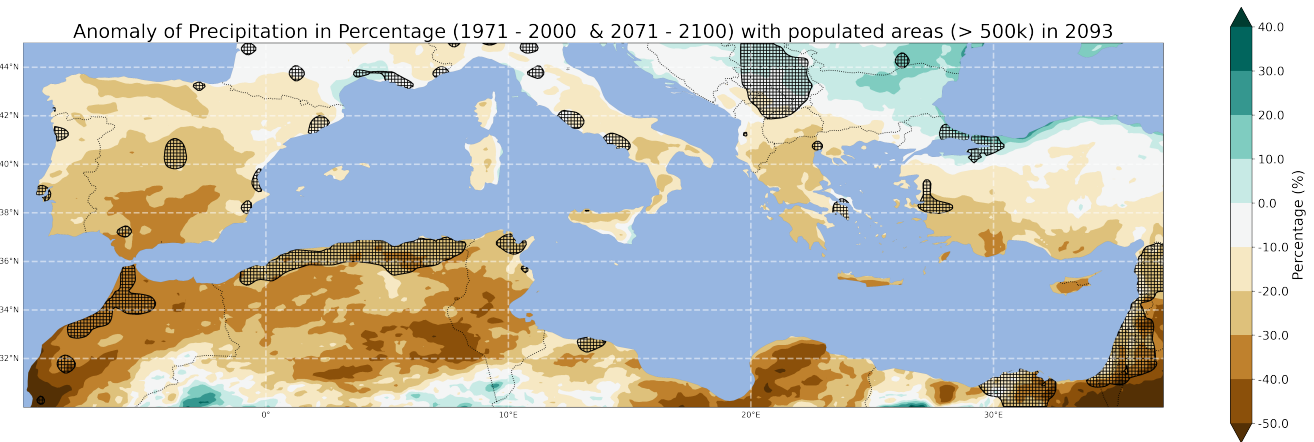


Figure 9: Percentage Anomaly of Yearly Average Precipitation (1971 - 2000 & 2071 - 2100) with Population Projection over 500,000 in 2093.

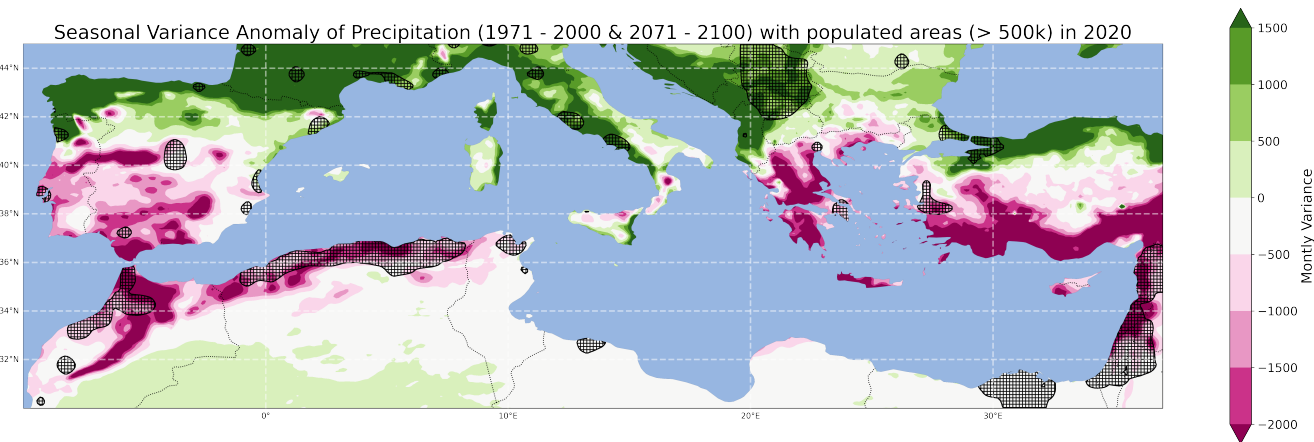


Figure 10: Seasonal Variance Anomaly of Precipitation (1971 - 2000 & 2071 - 2100) with Population Projection over 500,000 in 2093.

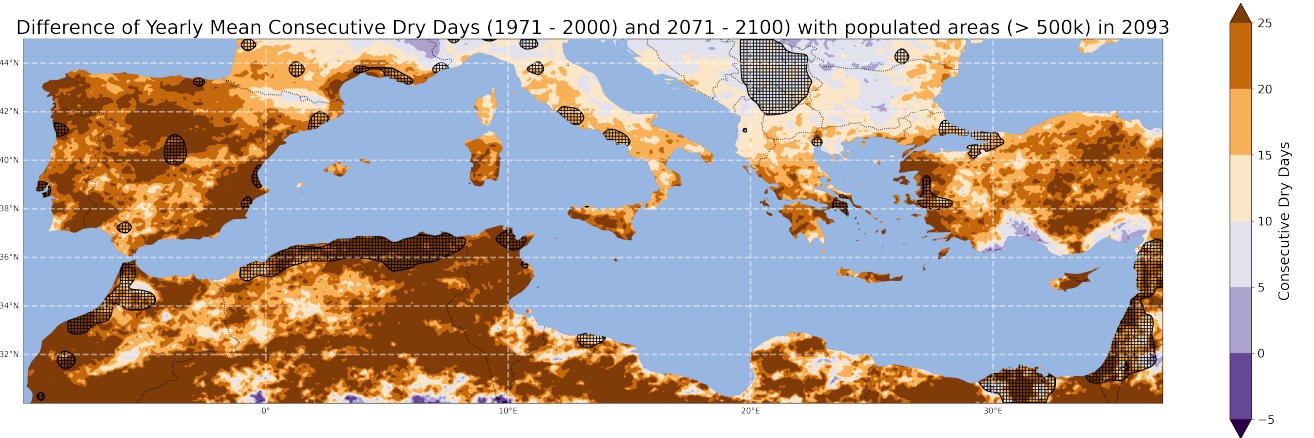


Figure 11: Difference in Yearly Consecutive Dry Days (1971 - 2000 & 2071 - 2100) with Population Projection over 500,000 in 2093.

4.3 Madrid, Spain.

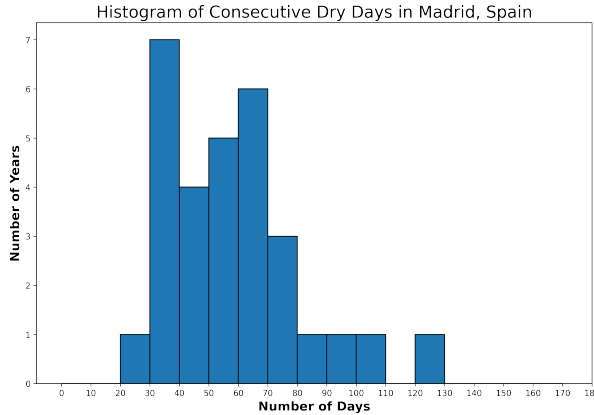


Figure 12: Histogram of CDDs (1971 - 2000).

Consecutive Dry Days (CDDs) of Madrid, Spain (Lat: 40.42 °; Lon: -03.70 °).

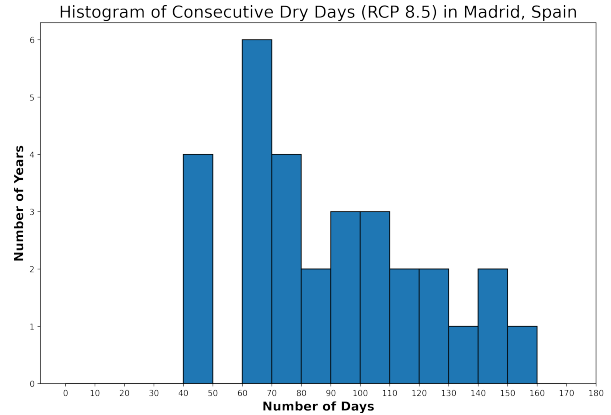


Figure 13: Histogram of CDDs (2071 - 2100).

Raincatching Water Ratio in Madrid, Spain

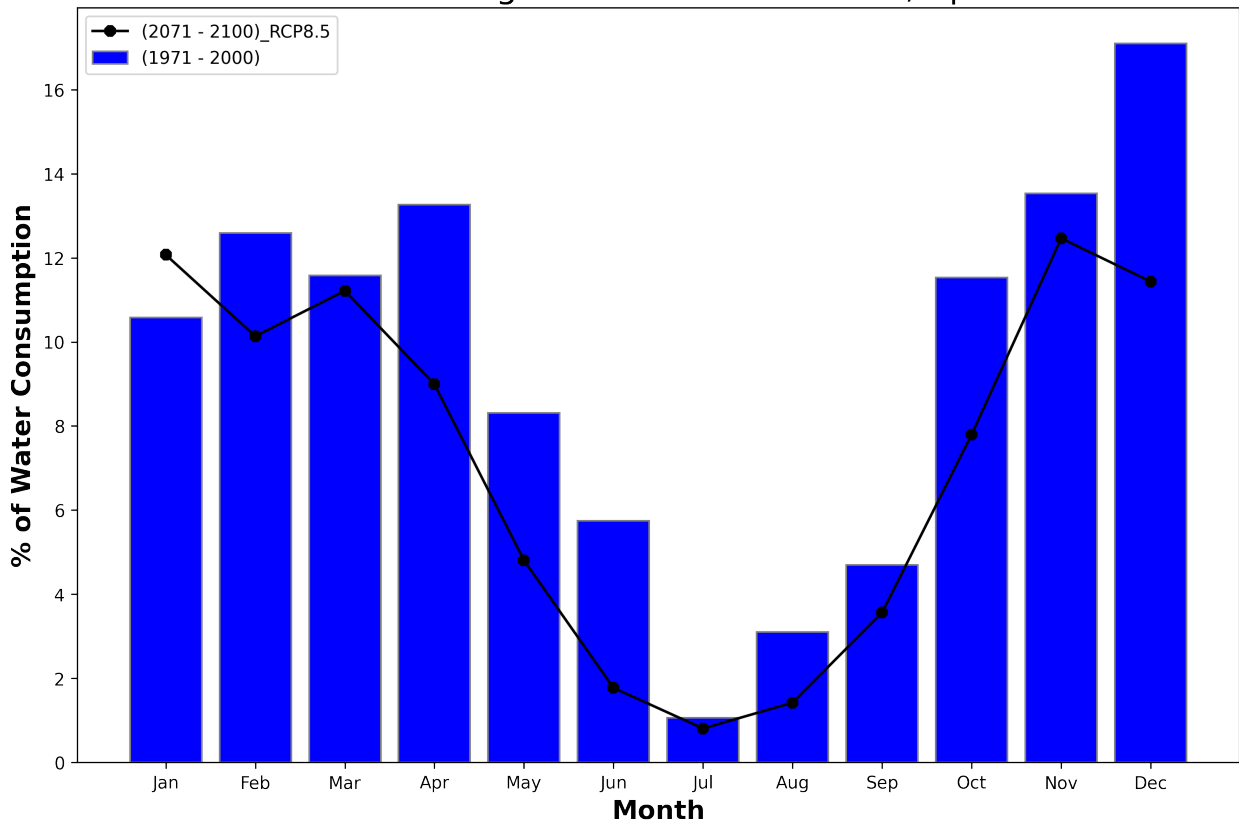


Figure 14: Potential Percentage of Domestic Water Consumption by Raincatching.

5 Discussion and Conclusion

As shown in Figure 3, the average rainfall is widely varied. We can find values larger than 1000 mm in the Northern Iberian Peninsula, Southern France, Northern Italy, and Eastern Balkans. On the other hand, highly arid areas such as Northern Africa, the Nile River Delta and some parts of the Middle East all have values of mean yearly precipitation under 100 mm. One of the characteristics of the Mediterranean Climate, according to *Köppen Climate Classification* (Köppen, 1936), is the annual rainfall regimen which has dry summers and wet winters; this can be observed in Figures 4 & 5. All of Southern Europe receives between 25 - 100 mm up

to more than 475 mm of rain in winter season contrary to summer.

This seasonal variance that exists in the average year is exemplified in Figure 6. However, as a general trend, the amount of precipitation and annual variance diminishes, especially south of the 36 ° parallel. The opposite holds true for the index of Consecutive Dry Days (Figure 7).

5.1 Current and Future Prospects for Rainwater Capture

The results from the radiative forcing of the RCP 8.5 scenario and its consequences on precipitation patterns in the Mediterranean coastline are unnerving. The contrast in Figures 9 & 10 demonstrates that overall (with a handful of exceptions), there will be less rain on average. A large portion of the map lost more than 50 mm of mean rainfall, particularly the Iberian Peninsula, North Africa, Italy, the Southern Balkans, Southern Turkey and the Middle East. The seasonal variance change is explained to 30.39 % by change in the amount of precipitation to significance level of $\alpha = 0.001$. Moreover, there is an increase of CDDs on average year is widely spread through out the region.

Practically all Spain sees a decrease in rainfall, representing between 10 to 40 % and increase in CDDs. Specifically, Madrid sees an average increase of 25 CDDs and a 20 to 30 % loss in mean rainfall. The median current of CDDs for Madrid is 30 to 40; meanwhile, for the future, the median shifts to 60 to 70 CDDs. Additionally the extreme of CDDs extend up to 160 CDDs during the period of (2071 - 2100). The implication that this has for rainwater harvesting is negative, as we can capture less water for the same area and increasingly time scattered manner. For reference, in fixed year, we could expect capture a 17 % of your domestic water consumption from rainfall in December (1971 - 2000). Unlike for the scenario RCP 8.5 where the maximum we can expect is up to 12 % for November and January.

Although the data concludes that building or adapting infrastructure dedicated to rainwater harvest will be less efficient in the future, for this reason alone, it should not be discarded. As there is no silver bullet solution to water stress, understanding that in the Mediterranean Basin water stress will only increase assuming conditions stay the same. Diversifying our sources from where we obtain water is necessary to fulfill our needs, given the future outlook.

References

- ESGF CORDEX (2022). Public cordex documents and lists for referencing in web sites. <https://is-enes-data.github.io/>.
- Instituto Nacional de Estadística de España (2018). Nota a la Prensa: Estadística sobre el suministro y saneamiento del agua.
- IPCC (2022). *Summary for Policymakers. In: Climate Change 2022: Mitigation of Climate Change. Con-*

tribution of Working Group III to the Sixth Assessment Report of the Intergovernmental Panel on Climate Change. Cambridge University Press, Cambridge, UK and New York, NY, USA.

Klein Goldewijk, K., Beusen, A., and Janssen, P. (2010). Long-term dynamic modeling of global population and built-up area in a spatially explicit way: Hyde 3.1. *The Holocene*, 20(4):565–573.

Kristensen, P., Lallana, C., Fribourg-Blanc, B., and Mortensen, L. (2004). Household water use: Background paper for eea report on household consumption and the environment. *Danish National Environmental Research Institute (NERI), European Topic Centre on Water, Roskilde*.

Köppen, W. (1936). *Das geographische System der Klimate*. Verlag von Gebrueder Borntraeger, Berlin.

Ouranos Inc., Logan, T., and contributors (2022). Icclim indices. xclim official documentation.
<https://xclim.readthedocs.io/en/stable/index.html>.

UN (2022). United nations, department of economic affairs: 68% of the world population projected to live in urban areas by 2050, says un. <https://www.un.org/development/desa/en/news/population/2018-revision-of-world-urbanization-prospects.html>.

WMO (2017). *WMO GUIDELINES ON THE CALCULATION OF CLIMATE NORMALS*. World Meteorological Organization Geneva, Switzerland.

Zhongming, Z., Linong, L., Xiaona, Y., Wangqiang, Z., Wei, L., et al. (2009). Water resources across europe—confronting water scarcity and drought.

6 Annex

6.1 RCP 8.5 Maps

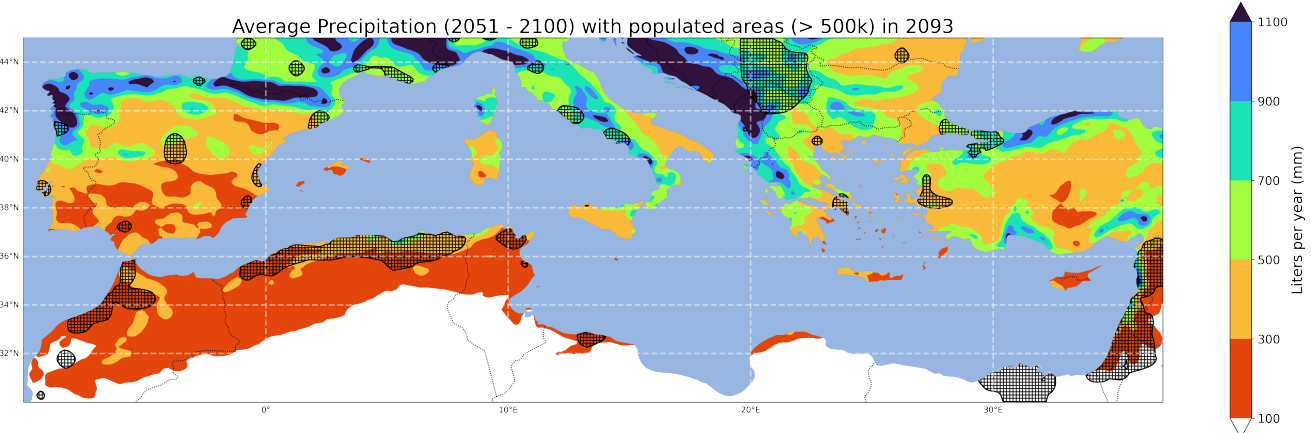


Figure 15: Yearly Average Precipitation (2071 - 2100) with Population Projection 2093.

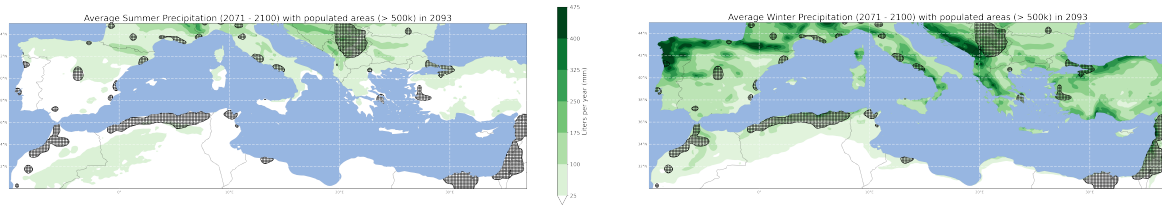


Figure 16: Average Summer Precipitation (2071 - 2100).

Summer (June, July and August) and Winter (December, January and February) for the Period (2071 - 2100) with Population Projection over 500,000 in 2093.

Figure 17: Average Winter Precipitation.

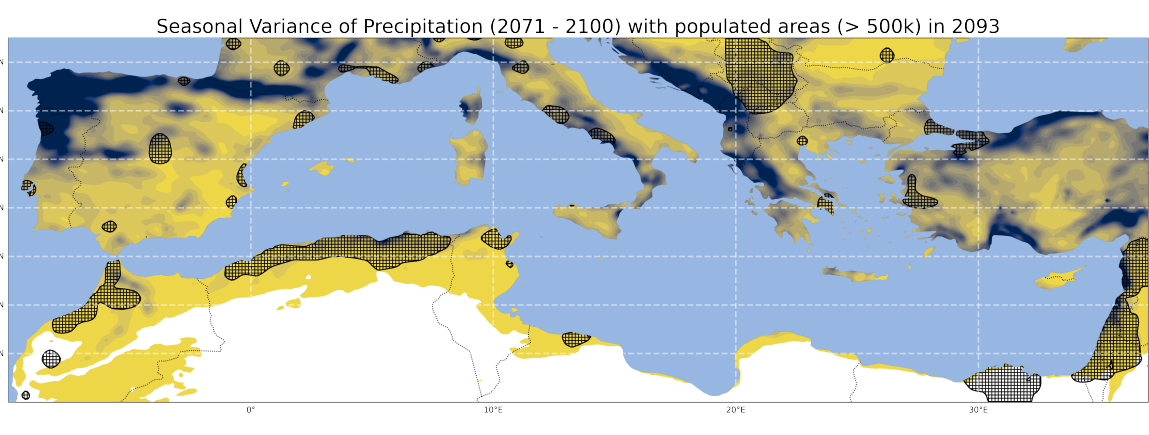


Figure 18: Average Seasonal Precipitation Variance (2071 - 2100) with Population Projection over 500,000 in 2093.

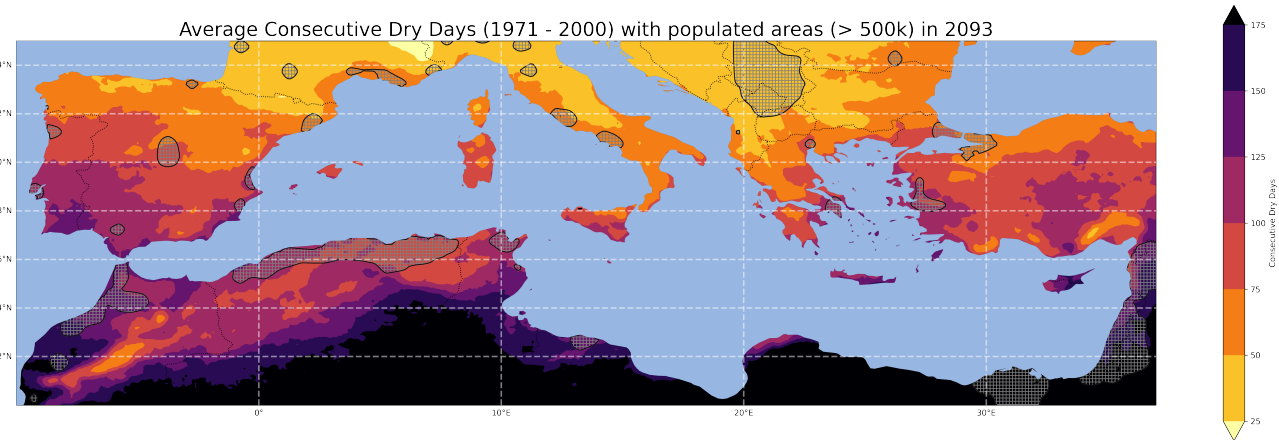


Figure 19: Average Consecutive Dry Days in a Year (2071 - 2100) with Population Projection over 500,000 in 2093.

6.2 Rome and Cairo

6.2.a) Histograms

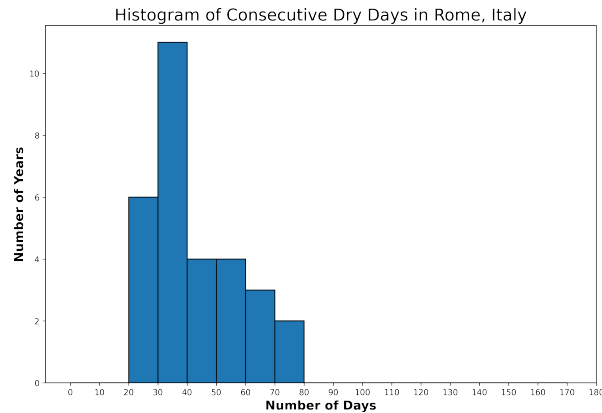


Figure 20: Histogram of CDDs (2071 - 2100).

Consecutive Dry Days (CDDs) of Rome, Italy (Lat: 41.89 °; Lon: 12.48 °).

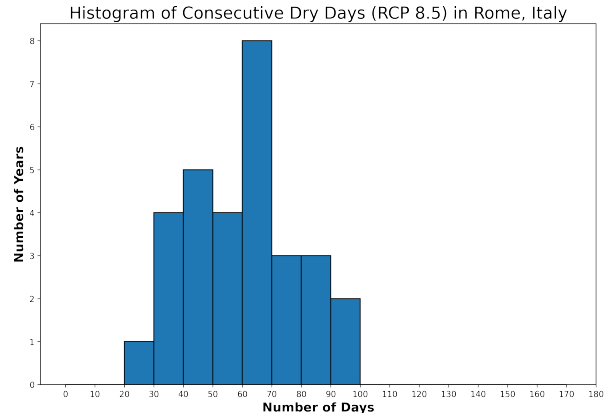


Figure 21: Histogram of CDDs (2071 - 2100).

Consecutive Dry Days (CDDs) of Rome, Italy (Lat: 41.89 °; Lon: 12.48 °).

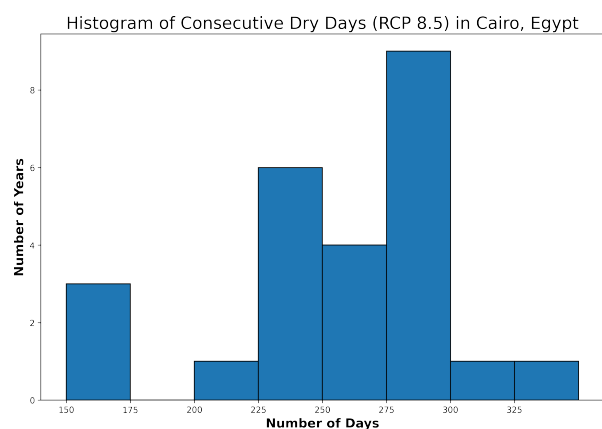


Figure 22: Histogram of CDDs (2071 - 2100).

Consecutive Dry Days (CDDs) of Cairo, Egypt (Lat: 30.04 °; Lon: 31.24 °).

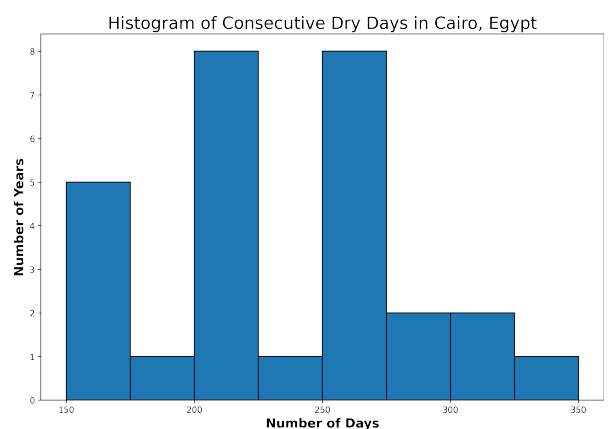


Figure 23: Histogram of CDDs (2071 - 2100).

Consecutive Dry Days (CDDs) of Cairo, Egypt (Lat: 30.04 °; Lon: 31.24 °).

6.2.b) Raincatcher

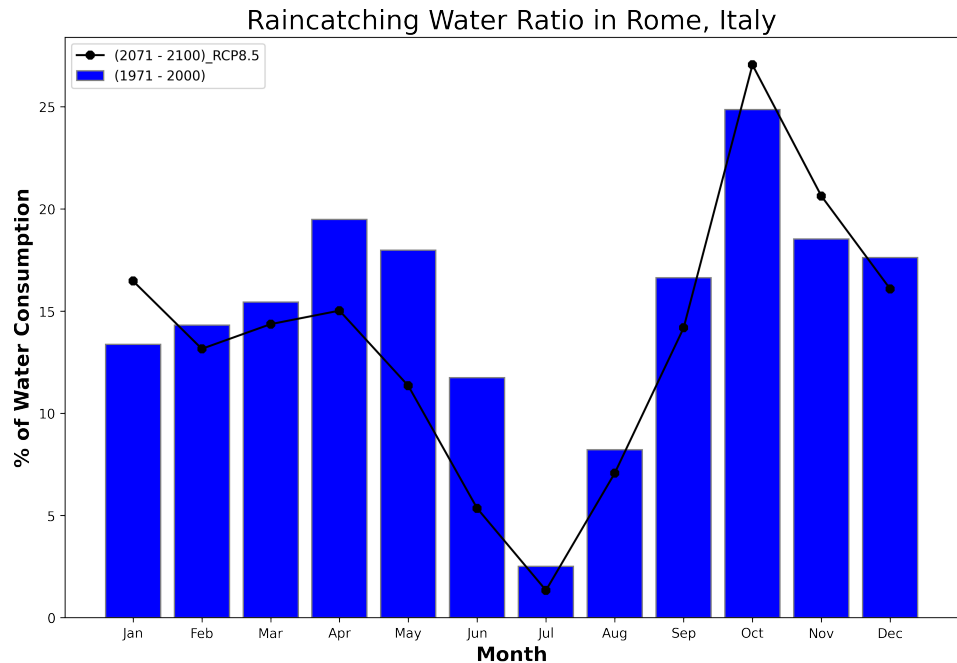


Figure 24: Potential Percentage of Domestic Water Consumption by Raincatching.

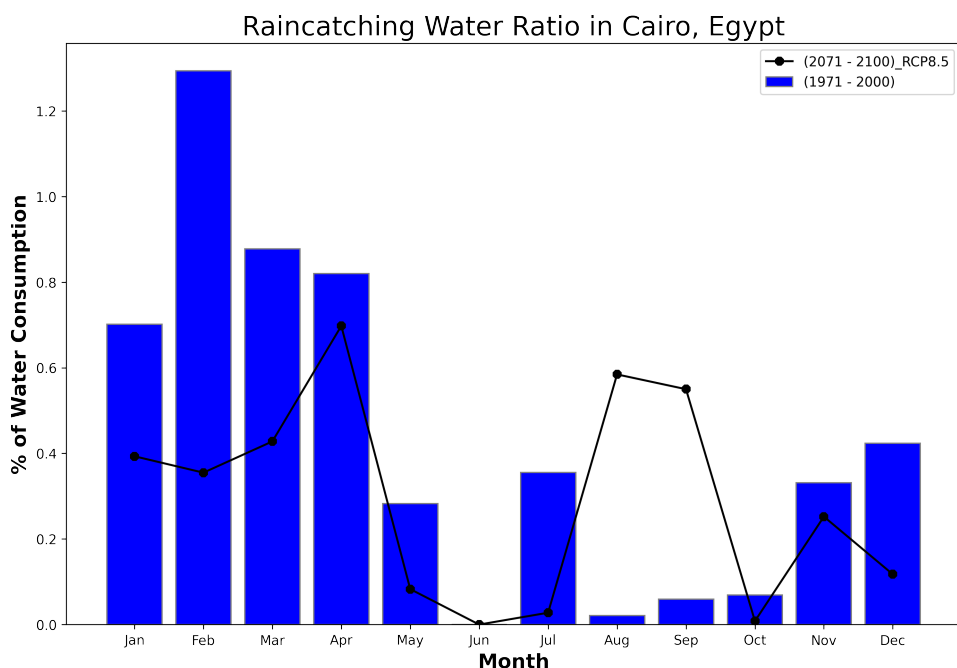


Figure 25: Potential Percentage of Domestic Water Consumption by Raincatching.